Chapter 3

IN VIVO AND IN VITRO DETECTION OF DOPAMINE D2 RECEPTORS IN UVEAL MELANOMAS

[1,5]Lisa Bodei, [2]Leo J. Hofland, [2,7]Diego Ferone, [3]Cornelia M. Mooy, [3]Johan M. Kros, [4]Dion A. Paridaens, [4]Seerp G. Baarsma, [6]Marco Ferdeghini, [2]Martin P. van Hagen, [1,2]Eric P. Krenning, and [1]Dik J. Kwekkeboom

Departments of [1]Nuclear Medicine, [2]Internal Medicine, and [3]Pathology, Erasmus University Medical Center Rotterdam (EMCR), Rotterdam, The Netherlands
[4]Eye Hospital, Rotterdam, The Netherlands
[5]Nuclear Medicine Division, European Institute of Oncology, Milan, Italy
[6]Department of Morphological-Biomedical Sciences, University of Verona, Italy
[7]Department of Endocrinological and Metabolic Sciences, University of Genoa, Genoa, Italy

Cancer Biotherapy & Radiopharmaceuticals 2003;18(6):895-902.

Abstract
Scintigraphy with radiolabeled benzamides was used in melanoma patients. Studies with a newer benzamide called ^{123}I-epidepride, a high-affinity D_2 receptor (D_2R) antagonist, showed high sensitivity in D_2R-positive pituitary adenomas. We evaluated the presence of D2R in patients with uveal melanomas *in vivo* with ^{123}I-epidepride, and *in vitro* in melanomas, using immunohistochemistry (IHC) and ^{125}I-epidepride autoradiography. We studied the *in vivo* tumor-to-background (TB) ratios in six patients with posterior uveal melanoma (one previously enucleated). IHC was performed in 3 of 6 tumors after enucleation and in another 20 uveal melanomas, 7 metastatic lymph nodes from skin melanoma, and 2 normal specimens. ^{125}I-epidepride autoradiography was performed in 10 uveal melanomas (3 of which were studied *in vivo*), 7 metastases, and 2 normal samples. Radioligand uptake was present in the affected eye of 5 patients with uveal melanoma (TB = 3.1–6.1) and absent in the operated one (TB = 1). Eight uveal tumors were positive at IHC (35%), 14 weakly positive (61%), and 1 negative (4%). Two metastases were positive (29%), 2 weakly positive (29%), and 3 negative (42%). Two uveal tumors were positive at autoradiography (20%), 7 had nonspecific binding (70%), and 1 was negative (10%). One metastasis was positive (14%), while 6 were negative (86%). ^{123}I-epidepride scintigraphy in uveal melanomas seems promising for sensitivity and image quality. D_2R was demonstrated in a significant proportion of the melanomas, although ^{123}I-epidepride uptake might also be nonspecific and unrelated to D_2R binding. Although further studies on larger series are needed, 123I-epidepride could represent a future tool to study the expression of D_2R in other classes of neuroendocrine tumors.

Introduction
Intraocular malignant melanoma is rare. The annual incidence is about six cases per million in the United States. Nevertheless, it is the most common primary intraocular malignancy, representing approximately 5% of all melanomas. The

most frequent presentation site (85%) is in the uvea. In contrast to cutaneous melanomas, uveal melanomas do not have direct access to lymphatic vessels, and therefore do not initially spread to regional lymph nodes. However, they do metastasize, usually to the liver, and this is the most common cause of death in patients with this type of melanoma. Therefore, early and adequate diagnosis and prompt therapy (i.e., radiotherapy or enucleation) is essential. Radiotracers that have been applied in uveal melanomas are *N*-isopropyl-p-[^{123}I]-iodoamphetamine (^{123}I-IMP)[1], ^{99m}Tc-glutathione [2,] ^{67}Gallium citrate [3], ^{99m}Tc-dimercaptosuccinic acid (DMSA) [4], monoclonal antibodies [5–8] and ^{18}F-FDG [9,10], as well as radiolabeled benzamides. Immunoscintigraphic techniques using ^{99m}Tc-labeled monoclonal IgG antibody against the high molecular weight melanoma antigen 225–28S showed a poor detection sensitivity (not exceeding 50%) in uveal melanomas, in both planar and single photon emission tomography (SPECT) studies [5,6], probably due to a different antigenic immunoreactivity [7]. The quality of this imaging technique was improved with a three-step pretargeting approach and high resolution SPECT [8] ^{18}F-FDG-positron emission tomography (PET) studies of uveal melanomas revealed variable glucose consumption among ocular lesions, [9,10], thus enabling the visualization only of some larger-sized lesions. PET tracers, such as ^{11}C-N-methylspiperone [11], possibly binding to melanin, are under investigation in ocular melanoma. Benzamide derivatives are dopamine D_2 receptor (D_2R) antagonists. They have been successfully applied in imaging of prolactin, growth–hormone-secreting and nonfunctioning pituitary adenomas, and in neurological and psychiatric disorders. ^{123}I-iodobenzamide (IBZM) SPECT has been used in pituitary adenomas with a varying detection sensitivity (< 60%), and a low tumor-tobackground (TB) ratio [12–15]. The newer dopamine receptor antagonist ^{123}I-epidepride, with a high affinity for D_2R (24–27 pM, in striatal and cortical postmortem tissue) shows a higher sensitivity (up to 100%), a better TB ratio, and is able to predict the response to dopamine agonist therapy [16]. ^{123}I-epidepride scanning was positive in 60% to 100% of nonfunctioning pituitary adenomas [16,17]. The ectodermic origin of melanocytes and the presence of melanin in the substantia nigra are the theoretical bases for the application of D_2R ligands, such as benzamides, in scintigraphic studies of patients with melanoma [18–22]. We therefore evaluated ^{123}I-epidepride in patients with uveal melanomas.

Materials and methods

Patients

Six patients with posterior uveal melanoma were studied with ^{123}I-epidepride. Five had newly diagnosed uveal melanoma, and one had had an enucleation, due to local tumor extension, with no further evidence of disease. The protocol was in accordance with the Helsinki Doctrine on Human Experimentation, and informed consent was obtained from the patients.

Methods

Scintigraphy protocol

^{123}I-epidepride was obtained from Dr. Peter Angelberger (Osterreichisches Forschungzentrum Seibersdorf GmbH, Seibersdorf, Austria, distributed by IDB Holland BV, Baarle-Nassau, The Netherlands). Patients were injected with 150

MBq ^{123}I-epidepride. Thyroid blockade was performed with 5 mL KI (1%) twice a day (b.i.d.), from the day before until the day after the study. SPECT images of the head were made 3 hours postinjection (p.i.) with a three-head γ-camera (Picker Prism 3000 XP, Picker International, Cleveland, OH), equipped with medium energy collimators. The pulse–height analyzer was centered over the energy peak (159 KeV, window width 20%). Acquisition parameters were 36 seconds/frame, 120 projections (40 steps of 3 grades each), 360° rotation, and 128 x 128 matrix. The tumor uptake was compared to the uptake in the basal ganglia and in the cerebral cortex, by means of semiquantitative evaluation: absent uptake degree 0; faint uptake, equal or less than the cerebral cortex, 1; higher than the cerebral cortex, 2; equal to or higher than the basal ganglia, 3. The TB ratio was also calculated, as a ratio of the mean count of the lesion over that of the cerebellum. Images were reconstructed by means of filtered backprojection (Ramp filter, Metz 4.84), and the attenuation was corrected by Chang algorithm (0.10 cm^{-1} attenuation coefficient). Total body images were also recorded 3 hours p.i., with a two-head camera (Prism 2000, Picker International), with an acquisition time of 40 minutes.

Immunohistochemistry protocol

Immunohistochemical analysis of D_2R was performed in three tumors after surgical enucleation. Twenty other uveal melanomas (from a pathology archive), as well as seven metastatic lymph nodes from seven different skin melanomas, and two normal specimens (skin and lymph nodes) were also studied. Four-micrometer (4 µm) paraffin-embedded sequential sections were deparafinized, rehydrated, exposed to microwave heating (in pH 6 citrate buffer, 15 minutes at 100°C), rinsed in tap water and phosphate-buffered saline (PBS), and incubated for 15 minutes in normal goat serum (1:10 dilution in PBS + 5% bovine serum albumin). The sections were then incubated overnight at 4°C with rabbit anti-D_2R polyclonal antibody (Chemicon International Inc., Temecula, CA), at 1:450 dilution. Finally, a standard streptavidinbiotinylated-alkaline phosphatase complex (Biogenix, San Ramon, CA) was used according to the manufacturer's instructions. To visualize bound antibodies, the sections were developed with New Fuchsine/Naphtol AS-MX, slightly counterstained with hematoxylin and mounted. Negative controls included omission of the primary antibody and preabsorbtion of the antibodies with immunizing receptor peptide (at a concentration of 6 µg/mL). Sections were evaluated using a semiquantitative arbitrary score: minus (-), absence of specific binding of the primary antibody; plus-minus (±), weak positivity; plus (+), clear positivity.

^{125}I-epidepride autoradiography

The *in vitro* binding of ^{125}I-epidepride was studied in 10 uveal melanomas (including the specimens from 3 patients already studied *in vivo* and by immunohistochemistry), 7 metastatic lymph nodes from 7 different skin melanomas, and 2 normal specimens. Twenty micrometer (20 µm) sections were mounted onto precleaned gelatin-coated microscope slides and stored at -80°C to improve the adhesion of tissue to the slides. The sections were preincubated at room temperature for 10 minutes in a buffer containing 50 mM Tris-HCl pH 7.7, 120 mM NaCl, 5 mM KCl, 2 mM $CaCl_2$, 1 mM $MgCl_2$, and 0.25% of ascorbic acid. The sections were then incubated for 60 minutes at room temperature in the same buffer, in the presence of ^{125}I-epidepride. Specific activity of the radioligand was high (approximately 2000 Ci/mmol). The sections were then washed twice for 10

minutes in buffer. After a short wash with distilled water, the sections were dried on air stream and exposed to Kodak Biomax Film (Amersham, Buckinghamshire, UK) or Hyperfilm-^{3}H (Amersham, Houten, The Netherlands) for 3–7 days in x-ray cassettes. Nonspecific binding was determined in an adjacent section in the presence of excess (1 μM) quinagolide, a non-ergot derivative D_2R agonist (Novartis, Basel, Switzerland). Sections of rat brain, obtained from the anterior part of the neostriatum (caudate nucleus/putamen), were taken as positive controls. A displacement curve of binding was performed by exposing these sections to decreasing concentrations of quinagolide (10^{-6}–10^{-13} M). Samples were considered positive when coincubation with 1 μM quinagolide displaced the ^{125}I-epidepride binding by more than 50%.

Results

^{123}I-epidepride Scintigraphy

No adverse reaction was observed in any of the patients studied. In all patients there was a high uptake in the basal ganglia. In all five patients who had a posterior uveal melanoma, the affected eye clearly showed increased radioligand uptake, whereas in the operated patient no pathological uptake was seen (Figs. 1 and 2). The TB ratio ranged between 3.1 and 6.1 in the affected eyes, whereas it was 1 in the operated patient and in the nonaffected eyes. The semiquantitative score was 2 in four patients, 1 in one patient (bearing a small uveal lesion sized 10 x 3 mm as measured by magnetic resonance imaging [MRI] scan), and 0 in the operated one. None of the patients had metastases, as recorded with computed tomography (CT) and/or MRI. Total body images during ^{123}I-epidepride scintigraphy did not show pathological uptake elsewhere in the body. The normal ^{123}I-epidepride biodistribution on the whole body scintigram was characterized by tracer uptake in the striatum, as well as in liver and gallbladder (the main excretory organs), intestines, and faintly in the lungs. The kidneys and urinary bladder were also visualized (Fig. 3).

D_2 Dopamine Receptor Immunohistochemistry

Results of the immunohistochemistry for D_2R are summarized in Tables 1 and 2, and some examples are shown in Figure 4. In total, 8 uveal tumors were positive (35%), 14 were weakly positive (61%), and 1 was negative (4%); 2 skin melanoma metastases were positive (29%), 2 were weakly positive (29%), and 3 were negative (42%).

^{125}I-epidepride Autoradiography

The results of autoradiography are shown in Tables 2 and 3. The binding was considered nonspecific when no displacement by an excess of quinagolide (1 μM) occurred. In total, two uveal tumors were positive (20%), seven had high nonspecific binding (70%), and one was negative (10%); one skin melanoma metastasis was positive (14%) and six were negative (86%). An overview of the *in vitro* results from the three patients previously scanned *in vivo* is shown in Table 4.

Discussion

Because melanocytes originate from the neural crest and melanin is present both in these cells and in the substantia nigra, benzamide derivatives have been proposed as radiopharmaceuticals for the staging of melanoma. Like sympathetic neurones, melanocytes take up tyrosine, oxidize it to 3,4-Dihydroxyphenylalanine (DOPA), and transform it to melanin. The exact mechanism of the binding of benzamides to melanoma cells remains unclear. Despite the finding of D_1R expression in B16 mouse melanoma cells, there is no evidence of G-coupled dopamine receptors in human melanocytes [23–25]. An intracellular binding of benzamides to melanin has been suggested since benzamide uptake is absent in amelanotic melanomas. Moreover, the uptake seems proportional to the melanin content and to the intracellular pH peak of melanin synthesis [26]. On the other hand, the binding of benzamides to sigma receptors, again with lack of visualization of amelanotic lesions [27], and possible involvement of the recently cloned dopamine receptor subtypes 3 and 4 cannot be ruled out [23]. The application of radiolabeled benzamides in uveal melanoma yielded a good detection sensitivity, ranging from 86% to 90%, compared to immunoscintigraphy [18,19]. In another study, an amelanotic lesion of the iris could not be visualized [20], corroborating the hypothesis of melanin uptake of the tracer, as suggested for cutaneous melanoma as well. Despite the limited number of patients evaluated in the present study, the results in the assessment of uveal melanoma lesions, in terms of imaging quality, specificity, and sensitivity (100% in our series) seem promising. As far as the mechanism of epidepride binding to melanoma tissue is concerned, using ^{125}I-epidepride autoradiography, we found a potential nonspecific binding to melanin in 7 out of 10 ocular melanomas and in 1 out of 7 metastatic lymph nodes. Conversely, two primary ocular melanomas and one metastatic lymph node showed specific ^{125}I-epidepride binding. According to immunohistochemistry, 8 out of 23 ocular melanomas (35%) and 2 out of 7 metastatic lymph nodes (29%) showed D_2R expression. Furthermore, the results of *in vivo* scintigraphy were in line with immunohistochemical evidence of D_2R expression in tumor samples. In favor of specific D_2R involvement in benzamide binding, an intriguing perspective is given by the outcome from the metastatic lymph nodes analyzed with immunohistochemistry. In fact, of two positive cases, one was an amelanotic metastasis. Thus, melanin cannot be considered the only explanation for benzamide binding in melanoma. These data are in agreement with those of literature from Larisch et al. [21] and Coenen et al. [26] who noticed that the binding of benzamides was dependent on the pH of the medium, peaking when the pH is optimal for melanin synthesis. Larisch et al. supposed that ^{123}I-IBZM does not bind to tyrosinase, as previously reported, because amelanotic melanomas also have this enzyme. Comparing the chemical similarities between benzamides and 5,6-dihydroxyindole (which is the direct precursor of melanin), and therefore the benzole ring and the pentangular ring containing a nitrogen atom, these authors hypothesized that ^{123}I-IBZM binds melanin, which derives from 5,6-dihydroxyindole polymerization.

Conclusions

We conclude that ^{123}I-epidepride uptake in malignant melanomas might be related to aspecific binding, although two proven techniques have clearly indicated the

presence of D_2R in a significant proportion of cases. Further studies on larger series are needed to correlate D_2R expression by immunohistochemistry to the histotype. Because ^{123}I-epidepride has been shown to demonstrate D_2R in pituitary adenomas as well as in some melanomas, it might represent a future tool to study D_2R expression in other classes of neuroendocrine tumors.

Acknowledgments
The authors thank Joke Zuijderwijk for her expert help in the laboratory.

References

1. Kotake F, Kawanishi M, Ishii I, et al. A case of choroidal malignant melanoma in which ^{123}I-IMP scintigraphy was useful for diagnosis. Kaku Igaku 1998;35:427.
2. Tutus A, Erkilic K, Ercan MT, et al. Scintigraphic visualization of ocular melanoma with Tc-99m glutathione. Ann Nucl Med 1997;11:143.
3. Ishii I, Tonami N, Nakajima K, et al. ^{67}Ga SPECT in the evaluation of orbital and ocular mass-like lesions. Nippon Igaku Hoshasen Gakkai Zasshi 1993;53:688.
4. Kiratli PO, Kiratli H, Ercan MT, Kostakoglu L. Visualization of uveal amelanotic melanoma with technetium-99m(V) dimercaptosuccinic acid. Ann Nucl Med 1997;11:147.
5. Brautigam P, Loeffler KU, Krause T, et al. Immunoscintigraphy with anti-225.28S for ocular mela-noma—A comparison with histology and immunohistochemistry. Nuklearmedizin 1997;36:42.
6. Loffler KU, Brautigam P, Simon J, et al. Immunoscintigraphy results in the comparison of ocular with cutaneous melanoma. Ophthalmology 1994;91:529.
7. Loffler KU, Simon JC, Wuttig C, et al. Antigen pattern in choroid melanoma in correlation with immunoscintigraphy. Ophthalmology 1995;92:723.
8. Magnani P, Paganeli G, Modorati G, et al. Quantitative comparison of direct antibody labeling and tumor pretargeting in uveal melanoma. J Nucl Med 1996;37:967.
9. Lucignani G, Paganelli G, Modorati G, et al. MRI, antibody-guided scintigraphy, and glucose metabolism in uveal melanoma. J Comput Assist Tomogr 1992;16:77.
10. Modorati G, Lucignani G, Landoni C, et al. Glucose metabolism and pathological findings in uveal melanoma: Preliminary results. Nucl Med Commun 1996;17:1052.
11. Sadzot B, Sheldon J, Flesher J, et al. Tracers for imaging melanin with positron emission tomography. Synapse 1999;31:5.
12. de Herder WW, Reijs AE, Kwekkeboom DJ, et al. In vivo imaging of pituitary tumours using a radiolabeled dopamine D_2 receptor radioligand. Clin Endocrinol (Oxf) 1996;45:755.
13. Ferone D, Lastoria S, Colao A, et al. Correlation of scintigraphic results using ^{123}I-methoxybenzamide with hormone levels and tumor size response to quinagolide in patients with pituitary adenomas. J Clin Endocrinol Metab 1998;83:248.
14. Colao A, Ferone D, Lastoria S, et al. Hormone levels and tumour size response to quinagolide and cabergoline in patients with prolactin-secreting and clinically non-functioning pituitary adenomas: Predictive value of pituitary scintigraphy with ^{123}I-methoxybenzamide. Clin Endocrinol (Oxf) 2000;52:437.
15. Ferone D, Pivonello R, Lastoria S, et al. In vivo and in vitro effects of octreotide, quinagolide and cabergoline in four hyperprolactinaemic acromegalics: Correlation with somatostatin and dopamine D_2 receptor scintigraphy. Clin Endocrinol (Oxf) 2001;154:469.
16. de Herder WW, Reijs AEM, de Swart J, et al. Comparison of iodine-123 epidepride and iodine-^{123}IBZM for dopamine receptor imaging in clinically nonfunctioning pituitary macroadenomas and macroprolactinomas. Eur J Nucl Med 1999;26:46.
17. Pirker W, Riedl M, Luger A, et al. Dopamine D_2 receptor imaging in pituitary adenomas using iodine-123–epidepride and SPECT. J Nucl Med 1996;37: 1931.

18. Bacin F, Michelot J, Bonafous J, et al. Clinical study of [^{123}I] N-(2-diethylaminoethyl)-4-iodobenzamide in the diagnosis of primary and metastatic ocular melanoma. Acta Ophthalmol Scand 1998;76:56.
19. Everaert H, Bossuyt A, Flamen P, et al. Visualizing ocular melanoma using iodine-123-N-(2-diethylaminoethyl) 4-iodobenzamide SPECT. J Nucl Med 1997;38:870.
20. Lodewijks H, Everaert H, Hennekes R, Bossuyt A. I-123–IDAB: A new tracer for scintigraphic visualisation of malignant melanoma. Bull Soc Belge Ophtalmol 1996;263:109.
21. Larisch R, Schulte KW, Vosberg H, et al. Differential accumulation of iodine-123–iodobenzamide in melanotic and amelanotic melanoma metastases in vivo. Nucl Med 1998;39:996.
22. Maffioli L, Mascheroni L, Mongioj V, et al. Scintigraphic detection of melanoma metastases with a radiolabeled benzamide ([Iodine-123]-(S)-IBZM. J Nucl Med 1994;35:1741.
23. Boni R, Steinert H, Boni RA, et al. Lack of expression of dopamine D2 receptors in malignant melanoma: Evidence for interaction of iodobenzofurans with melanin. Dermatology 1996;193:198.
24. Boni R, Lichtensteiger W, Steinert HC, et al. D1 dopamine receptors are not expressed in human melanoma. Melanoma Res 1997;7:117.
25. Chluba de Tapia J, Eberle AN. D1 dopamine receptor mRNA in B16 mouse melanoma cells. Ann NY Acad Sci 1993;680:660.
26. Coenen H.H., Brandau W, Dittmann H. Evaluation of melanoma-seeking N-(dialkylamino)-alkyl-[123,131-iodobenzamides by animal and cell culture studies. Lab Comp Radioph 1995;37:260.
27. Everaert H, Flamen P, Franken PR, et al. Sigma receptor imaging by means of 123-I-IDAB scintigraphy: Clinical application in melanoma and non small cell lung cancer. Anticancer Res 1997;17:1577.

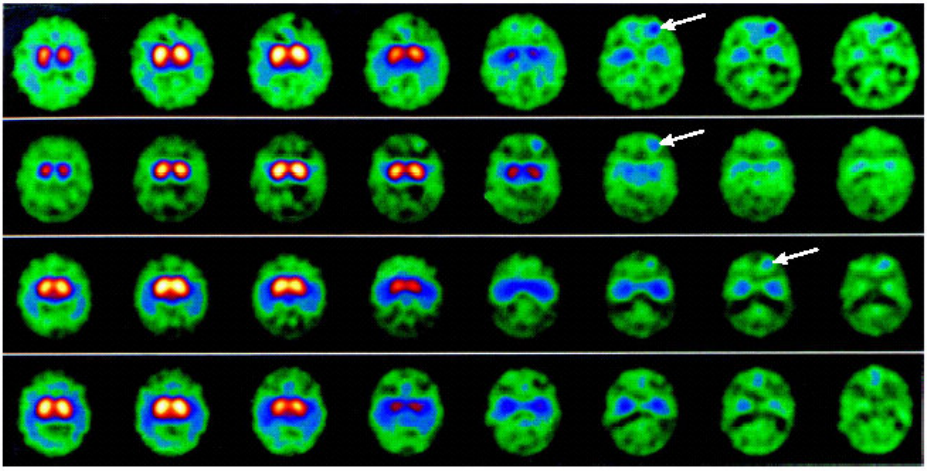

Figure 1. Transaxial slices from ^{123}I-epidepride SPECT in four of the studied patients. Note the pathological uptake in the affected eyes (first, second and third row, from patients C, A and B respectively), while no accumulation is seen in the operated patient (last row).

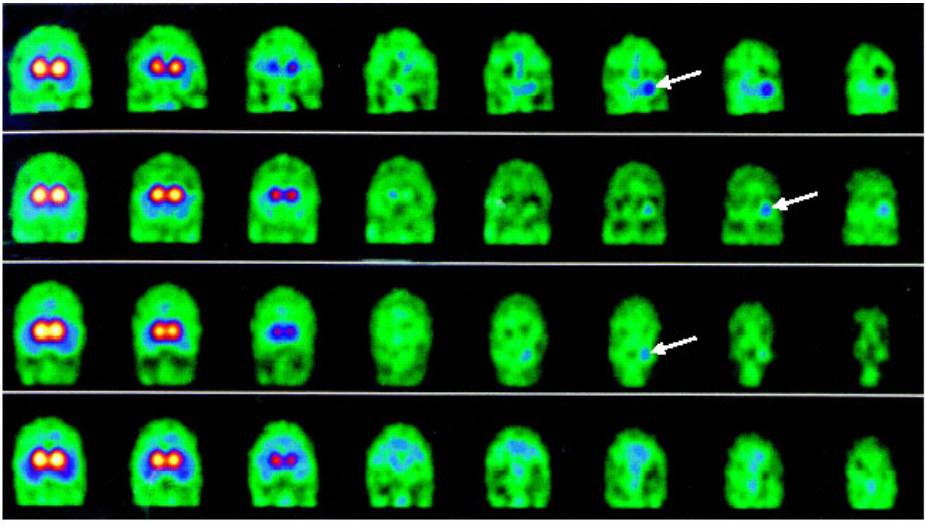

Figure 2. Coronal slices from ^{123}I-epidepride SPECT in four of the studied patients. Note the pathological uptake in the affected eyes (first, second and third row, from patients C, A and B respectively), while no accumulation is seen in the operated patient (last row).

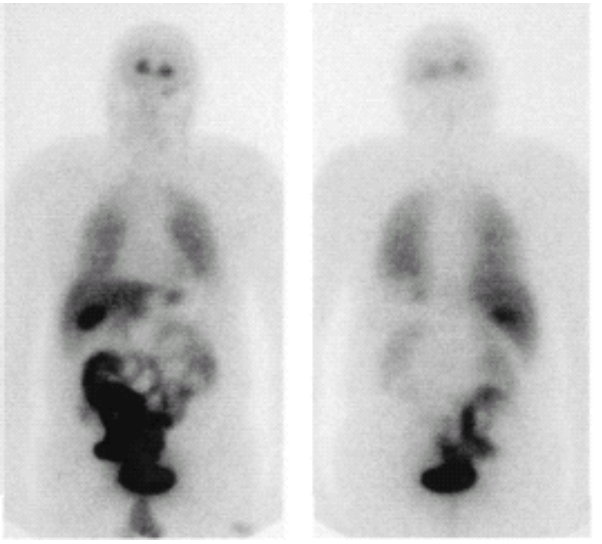

Figure 3. ^{123}I-epidepride total body images, anterior and posterior view (patient C). Note the accumulation in the affected eye (anterior projection) and the biodistribution features of the radioligand.

Table 1. Immunohistochemical Results in Uveal Melanoma Tissue Samples

	Uveal melanomas (n = *23*) *IHC*		
Histological type	−	±	+
Spindle cells	1	3	5
Epithelioid cells	0	4	1
Mixed	0	7	2
Total (%)	1 (4%)	14 (61%)	8 (35%)

Table 2. Histological, Immunohistochemical, and Autoradiographic Results in Non-Ocular Tissue Samples

Case no.	*Histology*	*IHC*	*Autoradiography*
1	Normal lymph node	–	–
2	Amelanotic metastasis	–	–
3	Amelanotic metastasis	+	+
4	Amelanotic metastasis	–	–
5	Amelanotic metastasis	–	–
6	Melanotic metastasis	+	+
7	Normal skin	+	+
8	Melanotic metastasis	+	+
9	Melanotic metastasis	+	–

IHC, immunohistochemistry

Table 3. Autoradiographic Results in Uveal Melanoma Tissue Samples

Uveal melanomas (n = 10)	*Autoradiography*	*Percent (%)*
7	Nonspecific	70
2	+	20
1	–	10

Table 4. Comparison Between *In Vivo* and *In Vitro* Results in Three Patients

Patient	*Melanotic lesion*	*IHC*	*In vitro binding*	*Scintigraphic T/B ratio*
A	yes	±	nonspecific	3.2
B	yes	+	nonspecific	3.1
C	yes	+	+	6.1

IHC, immunohistochemistry; TB, tumor to background